Frequency dependence of the penetration of electromagnetic fields through a small coupling hole in a thick wall

W-H. Cheng, A.V. Fedotov, and R.L. Gluckstern
Physics Department, University of Maryland, College Park, Maryland 20742
(Received 7 February 1995; revised manuscript received 19 April 1995)

We calculate a generalized polarizability and susceptibility for a circular hole in a thick metallic plate as a function of hole dimensions and wavelength. In particular, we construct a variational form that allows us to obtain accurate numerical results for the resonant frequency of a cavity with such a hole with a minimum of computational effort. Numerical results are obtained for a variety of hole dimensions relative to the wavelength. Results are also obtained analytically that are valid to second order in the ratio of the hole dimension to the wavelength for a vanishingly thin wall. These results are confirmed by the numerical calculations.

PACS number(s): 41.20.−q

I. INTRODUCTION

The penetration of electric and magnetic fields through a hole in a metallic wall plays an important role in many devices. In an accelerator, such holes in the beam pipe serve to allow access for pumping, devices for beam current and beam position measurement, coupling between cavities, etc. As a consequence, the beam generates wake fields in the beam pipe when it passes by such holes and these wake fields are capable of affecting beam quality and stability. In all these and other similar situations, the quantities of importance are the polarizability and the susceptibilities of such holes, quantities that also enter into the scattering of electromagnetic waves by holes in a metallic screen [1]. In much of the early work the hole dimensions were considered to be very small compared to the wavelength.

The purpose of this paper is to extend the calculation to include the effects of finite wavelength, although we still confine our attention to wavelengths no smaller than the primary hole dimensions. For example, when considering the coupling impedance of a hole in the wall of a beam pipe [2] of rectangular cross section, we must evaluate the integral over the hole

$$I = \int\int_{\text{hole}} dxdy \left[E_x^{(2)} H_y^{(1)} - E_y^{(2)} H_x^{(1)}\right] \tag{1.1}$$

at the inner surface of the beam pipe. Here the normal to the wall is in the z direction, the superscript (1) refers to the fields with no hole, and the superscript (2) refers to the fields in the presence of the hole.

The integral in Eq. (1.1) is exactly the same as the coupling integral used to describe the coupling between waveguides and/or cavities [3, 4]. In fact it is also the integral that describes the detuning of a cavity by a hole in a plane cavity wall as shown in Sec. IV, with the superscripts (1) and (2) having the same meaning. It is therefore reasonable to relate the frequency dependence of the coupling impedance in Eq. (1.1) to the detuning of the cavity by a hole whose dimensions may be as large as the wavelength. In this paper we show how to obtain the detuning of a cavity by a hole in the wall without assuming an infinite wavelength.

The conventional treatment of Eq. (1.1) proceeds by way of the polarizability and susceptibilities of the hole in the wall [1, 3, 4]. By redefining these parameters in terms of the cavity detuning we construct a generalized polarizability and susceptibility. In this way, we include the frequency dependence of the polarizability and susceptibility as well as the contributions of higher multipole moments of the hole, as discussed in Sec. IV. But these generalized polarizabilities and susceptibilities should only be seen as intermediate vehicles to relate the coupling integrals of interest to the detuning of the cavity by the hole.

We now define the generalized polarizability and susceptibility by means of the detuning of the modes of the symmetric cavity structure shown in Fig. 1 due to the presence of the hole. Clearly the modes will be either symmetric or antisymmetric in the axial coordinate. We will obtain an expression for the detuning of the pillbox cavity of length L and radius b due to the presence of the hole. Our analysis will be limited to the modes near the $\mathrm{TM}_{0N\ell}$, $\mathrm{TM}_{1N\ell}$, and $\mathrm{TE}_{1N\ell}$ modes of the unperturbed pillbox.

II. GENERAL ANALYSIS

Our analysis can be generalized to include cavity regions and iris regions of arbitrary cross section. Taking $z_1 = 0$ to be the left end of the left cavity, we can write the transverse electric field as

$$\boldsymbol{E}_\perp^{(C)}(\boldsymbol{r}, z_1) = \sum_n a_n \boldsymbol{e}_n(\boldsymbol{r}) \frac{\sin\beta_n z_1}{\sin\beta_n L}, \tag{2.1}$$

where $\boldsymbol{r}$ stands for the transverse coordinates x and y and the modes $\boldsymbol{e}_n$ may be either TM or TE. Here

$$\beta_n^2 = k^2 - \gamma_n^2, \tag{2.2}$$

where γ_n^2 are the eigenvalues of the two-dimensional scalar Helmholtz equation in the cavity region with the

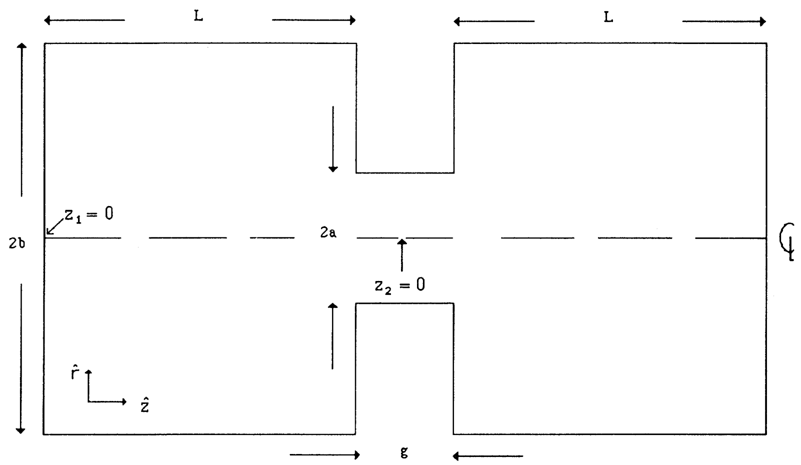

FIG. 1. Schematic diagram of two cavities coupled by an iris.

appropriate boundary conditions. We use latin subscripts (n, m, N, etc.) for the cavity region and $kc/2\pi$ is the frequency.

The transverse electric field in the iris region can similarly be written as

$$\boldsymbol{E}_{\perp}^{(I)}(\boldsymbol{r}, z_2) = \sum_{\nu} b_{\nu} \boldsymbol{e}_{\nu}(\boldsymbol{r}) \frac{\cos\beta_{\nu} z_2}{\cos\beta_{\nu} g/2}, \tag{2.3}$$

where $z_2 = 0$ is now the center of the iris region and where we use greek subscripts (ν, μ, σ, etc.) for the iris region. Equation (2.3) is appropriate for the modes in our symmetric structure for which $\boldsymbol{E}_{\perp}^{(I)}$ is even in z_2. For those modes where $\boldsymbol{E}_{\perp}^{(I)}$ is odd in z_2 we need to replace the cosines by sines in Eq. (2.3).

We now express the coefficients a_n and b_{ν} in terms of $\boldsymbol{E}_{\perp}(\boldsymbol{r}) \equiv \boldsymbol{u}(\boldsymbol{r})$ at the interface between the cavity and the iris ($z_1 = L$, $z_2 = -g/2$). Since $\boldsymbol{e}_n$ and $\boldsymbol{e}_{\nu}$ are complete orthonormal sets, we find

$$a_n = \int_{S_1} dS\ \boldsymbol{u} \cdot \boldsymbol{e}_n\ ,\ b_{\nu} = \int_{S_1} dS\ \boldsymbol{u} \cdot \boldsymbol{e}_{\nu}, \tag{2.4}$$

where S_1 is the cross section of the iris and we use the fact that $\boldsymbol{E}_{\perp} = \boldsymbol{0}$ on the iris surface at $z_1 = L$.

The transverse magnetic field in each region can be written as [we use the time dependence $\exp(jkct)$]

$$Z_0 \boldsymbol{H}_{\perp}^{(C)} \times \hat{\boldsymbol{z}} = j \sum_{n} \lambda_n a_n \boldsymbol{e}_n(\boldsymbol{r}) \frac{\cos\beta_n z_1}{\sin\beta_n L}, \tag{2.5}$$

$$Z_0 \boldsymbol{H}_{\perp}^{(I)} \times \hat{\boldsymbol{z}} = -j \sum_{\nu} \lambda_{\nu} b_{\nu} \boldsymbol{e}_{\nu}(\boldsymbol{r}) \frac{\sin\beta_{\nu} z_2}{\cos\beta_{\nu} g/2}, \tag{2.6}$$

where

$$\lambda_n = \frac{Z_0}{Z_n} = \begin{cases} k/\beta_n\ , & \text{TM} \\ \beta_n/k\ , & \text{TE,} \end{cases}$$

$$\lambda_{\nu} = \frac{Z_0}{Z_{\nu}} = \begin{cases} k/\beta_{\nu}\ , & \text{TM} \\ \beta_{\nu}/k\ , & \text{TE,} \end{cases} \tag{2.7}$$

with Z_n being the impedance of the "cavity" waveguide and Z_{ν} being the impedance of the "iris" waveguide. Here $Z_0 = \sqrt{\mu_0/\epsilon_0}$ is the impedance of free space and

$$\beta_{\nu}^2 = k^2 - \gamma_{\nu}^2, \tag{2.8}$$

where γ_{ν}^2 are the eigenvalues of the two-dimensional scalar Helmholtz equation with the appropriate boundary conditions in the iris region. Equating the transverse magnetic field at $z_1 = L, z_2 = -g/2$ in the region S_1 leads to the integral equation for the unknown function $\boldsymbol{u}(\boldsymbol{r})$

$$\int_{S_1} dS'\ \boldsymbol{u}(\boldsymbol{r}') \cdot \overleftrightarrow{K}(\boldsymbol{r}, \boldsymbol{r}') = \boldsymbol{0}, \tag{2.9}$$

where

$$\overleftrightarrow{K}(\boldsymbol{r}, \boldsymbol{r}') = \sum_{n} \lambda_n \boldsymbol{e}_n(\boldsymbol{r}) \boldsymbol{e}_n(\boldsymbol{r}') \cot\beta_n L - \sum_{\nu} \lambda_{\nu} \boldsymbol{e}_{\nu}(\boldsymbol{r}) \boldsymbol{e}_{\nu}(\boldsymbol{r}') \tan\beta_{\nu} g/2. \tag{2.10}$$

III. VARIATIONAL FORM FOR THE FREQUENCY

Let us multiply Eq. (2.9) by $\boldsymbol{u}(\boldsymbol{r})$ and integrate over dS in the region S_1. This leads to

$$\sum_{n} \lambda_n \cot\beta_n L \left[\int dS\ \boldsymbol{u} \cdot \boldsymbol{e}_n\right]^2 - \sum_{\nu} \lambda_{\nu} \tan(\beta_{\nu} g/2) \left[\int dS\ \boldsymbol{u} \cdot \boldsymbol{e}_{\nu}\right]^2 = 0. \tag{3.1}$$

We now consider Eq. (3.1) as a transcendental equation for the frequency k in terms of the yet to be determined $\boldsymbol{u}(\boldsymbol{r})$, which we write symbolically as

$$F(k, \boldsymbol{u}(\boldsymbol{r})) = 0. \tag{3.2}$$

Any change of $\boldsymbol{u}(\boldsymbol{r})$ will lead to a change in k that satisfies

$$\frac{\partial F}{\partial k} \delta k = -\frac{\partial F}{\partial \boldsymbol{u}} \delta \boldsymbol{u}. \tag{3.3}$$

The requirement that Eq. (3.1) be an extremum for k requires that the first-order variation with respect to $\delta \boldsymbol{u}$ must vanish. But this variation leads to the requirement that $\boldsymbol{u}(\boldsymbol{r})$ must satisfy Eq. (2.9). Thus Eq. (3.1) can be thought of as a variational equation for the frequency, which is an extremum when $\boldsymbol{u}(\boldsymbol{r})$ is the correct function.

We shall implement this statement by expanding $\boldsymbol{u}(\boldsymbol{r})$ into a complete set $\boldsymbol{f}_\nu(\boldsymbol{r})$ in the region S_1. Specifically we write

$$\boldsymbol{u}(\boldsymbol{r}) = \sum_\nu c_\nu \boldsymbol{f}_\nu(\boldsymbol{r}) \tag{3.4}$$

and obtain

$$\lambda_N \cot \beta_N L \left(\sum c_\nu K_{N\nu} \right)^2 = \sum_\nu \sum_\mu c_\nu c_\mu M_{\nu\mu}, \tag{3.5}$$

where $M_{\nu\mu}$ is a symmetric matrix defined by

$$M_{\nu\mu} = - \sum_{n \neq N}{}' \lambda_n \cot \beta_n L \; K_{n\mu} K_{n\nu} + \sum_\sigma \lambda_\sigma \tan(\beta_\sigma g/2) \; K_{\sigma\mu} K_{\sigma\nu}. \tag{3.6}$$

Here

$$K_{n\nu} \equiv \int_{S_1} dS \; \boldsymbol{e}_n \cdot \boldsymbol{f}_\nu \; , \; K_{\sigma\nu} \equiv \int dS \; \boldsymbol{e}_\sigma \cdot \boldsymbol{f}_\nu. \tag{3.7}$$

Note that we have separated the term $n = N$ and moved it to the left-hand side of Eq. (3.5) since we shall be looking at modes close to the cavity modes corresponding to $\beta_N L = \ell\pi$ or

$$k_{N\ell}^2 = \frac{\ell^2 \pi^2}{L^2} + \gamma_N^2, \tag{3.8}$$

where ℓ is an integer. As a matter of fact, for a small iris hole, the sum on the right-hand side of Eq. (3.5) diverges inversely as the cube of the iris hole dimensions, leading to the cavity modes corresponding to Eq. (3.8) when the iris hole disappears.

We now consider Eq. (3.5) as a variational statement requiring that

$$\sum_\nu \sum_\mu c_\nu c_\mu M_{\nu\mu} = \mathcal{E} \tag{3.9}$$

(where $\mathcal{E}$ denotes the extremum) subject to the arbitrary normalization constraint

$$\sum c_\nu K_{N\nu} = 1. \tag{3.10}$$

The method of Lagrange multipliers leads directly to the matrix equation

$$\sum_\mu M_{\nu\mu} c_\mu = \alpha K_{N\nu}, \tag{3.11}$$

where -2α is the Lagrange multiplier. The solution of Eq. (3.11) for c_ν is

$$c_\nu = \alpha \sum_\mu (\boldsymbol{M}^{-1})_{\nu\mu} K_{N\mu}, \tag{3.12}$$

leading directly to the equation for the frequency

$$\frac{\tan \beta_N L}{\lambda_N} = \sum_\nu \sum_\mu K_{N\nu} (\boldsymbol{M}^{-1})_{\nu\mu} K_{N\mu}. \tag{3.13}$$

Since the frequency k is also contained in the parameters $\beta_n, \beta_\nu, \beta_\mu$, and β_σ in $M_{\nu\mu}$, Eq. (3.13) must be solved by iteration, each successive value of k coming from the left-hand side using the preceding k on the right-hand side.

IV. POLARIZABILITY AND SUSCEPTIBILITY

We now apply the considerations usually used [1, 3, 5] when a hole is placed in a cavity wall. We define the orthonormal cavity modes for the cavity on the left-hand side (without the hole) by

$$\nabla \times \boldsymbol{E}_m = k_m \boldsymbol{H}_m, \quad \nabla \times \boldsymbol{H}_m = k_m \boldsymbol{E}_m \tag{4.1}$$

and write the cavity "voltage" and "current" in the mth mode as

$$V_m = \int \boldsymbol{E} \cdot \boldsymbol{E}_m dv, \quad I_m = \int \boldsymbol{H} \cdot \boldsymbol{H}_m dv, \tag{4.2}$$

where the integration is over the volume of the cavity on the left-hand side in Fig. 1. Here $\boldsymbol{E}, \boldsymbol{H}$ are the fields in the presence of the hole. We now use Maxwell's equations to obtain

$$Z_0 k_m I_m = jk V_m,$$

$$k_m V_m = -jk Z_0 I_m - \int dS \; \boldsymbol{n} \cdot \boldsymbol{E} \times \boldsymbol{H}_m, \tag{4.3}$$

where the surface integral is over the hole opening in the wall. The resulting equation for V_m is

$$(k^2 - k_m^2) V_m = k_m \int_{\text{hole}} dS \; \boldsymbol{n} \cdot \boldsymbol{E} \times \boldsymbol{H}_m. \tag{4.4}$$

The right-hand side of Eq. (4.4) is usually approximated by using the static analysis for the fields near the hole. This leads to a form involving the induced electric and magnetic dipole moments

$$p_z = \int \int_{\text{hole}} dxdy \; xE_x = \int \int_{\text{hole}} dxdy \; yE_y \tag{4.5}$$

and

$$m_x = - \int \int_{\text{hole}} dxdy \; xH_z,$$

$$m_y = - \int \int_{\text{hole}} dxdy \; yH_z, \tag{4.6}$$

where the direction $\hat{\boldsymbol{z}}$ is normal to the hole surface. Specifically we find

$$(k^2 - k_m^2) V_m = k_m^2 \boldsymbol{p} \cdot \boldsymbol{E}_m(0) - jkk_m Z_0 \boldsymbol{m} \cdot \boldsymbol{H}_m(0), \tag{4.7}$$

where $\boldsymbol{E}_m(0)$ is the normalized electric field normal to the hole and $\boldsymbol{H}_m(0)$ is the normalized magnetic field tangential to the hole at the hole location in the absence of the hole. If we define the polarizability (a scalar) and susceptibility (a 2×2 tensor) as

$$\boldsymbol{p} = \chi \boldsymbol{E}, \quad \boldsymbol{m} = \overset{\leftrightarrow}{\psi} \cdot \boldsymbol{H} \tag{4.8}$$

and assume that mode M dominates so that $\boldsymbol{E} \cong V_M \boldsymbol{E}_M, \boldsymbol{H} \cong I_M \boldsymbol{H}_M$, we find

$$k^2 - k_M^2 = k_M^2 E_M^2(0)\chi - k^2 \boldsymbol{H}_M(0)\cdot \overset{\leftrightarrow}{\psi} \cdot \boldsymbol{H}_M(0). \tag{4.9}$$

In Eq. (4.9) we must use the symmetric or antisymmetric values $\chi_{s,a}, \psi_{s,a}$ depending on the symmetry of the excitation of the two cavities.

Let us now examine the integral in Eq. (4.4) in greater depth for a $\mathrm{TM}_{0N\ell}$ mode. The magnetic field $\boldsymbol{H}_m$, with no hole, has only a θ component in the plane of the hole, which is proportional to

$$H_{m\theta} = C J_1(s_N r/b), \tag{4.10}$$

where s_N is the Nth zero of $J_0(s) = 0$. The rectangular components of $H_{m\theta}$ are

$$H_x = -C \sin\theta J_1\left(\frac{s_N r}{b}\right) = -\frac{C s_N}{b}\left[y - \frac{s_N^2(x^2+y^2)y}{8} + \cdots\right], \tag{4.11}$$

$$H_y = C \cos\theta J_1\left(\frac{s_N r}{b}\right) = \frac{C s_N}{b}\left[x - \frac{s_N^2(x^2+y^2)x}{8} + \cdots\right]. \tag{4.12}$$

Using this expansion, the coupling integral becomes, apart from the overall constant Cs_N/b,

$$\int_{\text{hole}} dS\, \boldsymbol{n}\cdot \boldsymbol{E}\times \boldsymbol{H}_m = \iint_{\text{hole}} dx dy (xE_x + yE_y) - \frac{s_N^2}{8}\iint_{\text{hole}} dx dy (xE_x + yE_y) \times (x^2+y^2) + \cdots. \tag{4.13}$$

The first term on the right-hand side of Eq. (4.13) is twice the electric dipole moment, according to Eq. (4.5). However, since E_x and E_y are the exact solutions in the presence of a hole, this term is expected to depend on the wave number k. But Eq. (4.13) also has an electric sextupole term, proportional to s_N^2, which will also have a k dependence in general. Therefore when we generalize χ in Eq. (4.9) to have a frequency dependence, this generalization will include all higher multipoles as well as the frequency dependence of each multipole. The argument applies as well to the susceptibilities by way of the $\mathrm{TM}_{1N\ell}$ and $\mathrm{TE}_{1N\ell}$ modes.

We therefore generalize the concept of the static polarizability by considering a mode that has a normal electric field, but no tangential magnetic field at the center of the hole (for example, the $\mathrm{TM}_{0N\ell}$ mode) and define a generalized polarizability as

$$\chi \equiv \frac{k^2 - k_M^2}{k_M^2 E_M^2(0)}. \tag{4.14}$$

Similarly we define a generalized susceptibility for a circular hole (for example, the $\mathrm{TM}_{1N\ell}$ or $\mathrm{TE}_{1N\ell}$ mode)

$$\psi \equiv \frac{k_M^2 - k^2}{k^2 H_M^2(0)}. \tag{4.15}$$

We envision k being calculated from Eq. (3.13) and χ or ψ being obtained for that frequency from Eq. (4.14) or (4.15). Clearly the mode identification M corresponds to three eigenvalues; that is, M stands for $0N\ell$ or $1N\ell$ as appropriate.

From this point on, χ and ψ should always be understood to be the generalized polarizability and susceptibility, even though this may not always be stated explicitly.

V. GENERALIZED POLARIZABILITY FOR A CIRCULAR IRIS HOLE

We now specialize to TM_{0n} waveguide modes in a circular geometry in order to obtain the polarizability [6]. The cavity radius is b and the iris radius is a and we use the complete set

$$\boldsymbol{f}_\nu(\boldsymbol{r}) = \boldsymbol{e}_\nu(\boldsymbol{r}) = -\boldsymbol{\nabla}\phi_\nu(r), \tag{5.1}$$

with

$$\phi_n(r) = \frac{J_0(s_n r/b)}{\sqrt{\pi} s_n J_1(s_n)}, \quad \phi_\nu(r) = \frac{J_0(s_\nu r/a)}{\sqrt{\pi} s_\nu J_1(s_\nu)}. \tag{5.2}$$

Here $s_{n,\nu}$ are the roots of the equation $J_0(s_{n,\nu}) = 0$. The integrals in Eq. (3.7) are

$$K_{n\nu}^{\chi} = \frac{2a^2 s_n J_0(s_n a/b)}{b^2 J_1(s_n)[s_\nu^2 - (s_n a/b)^2]}, \quad \gamma_n = \frac{s_n}{b} \tag{5.3}$$

and

$$K_{\sigma\nu}^{\chi} = \delta_{\sigma\nu}, \tag{5.4}$$

where the superscript χ denotes the polarizability. The matrix element in Eq. (3.6) becomes

$$M_{\nu\mu}^{\chi} = \delta_{\nu\mu}\frac{k}{\beta_\nu}\tan\frac{\beta_\nu g}{2} - {\sum_{n\neq N}}' \frac{k}{\beta_n}\cot\beta_n L\, K_{n\nu}^{\chi} K_{n\mu}^{\chi}. \tag{5.5}$$

The frequency can now be calculated using Eq. (3.13) and the symmetric polarizability using Eq. (4.14). The asymmetric polarizability is obtained by replacing $\tan(\beta_\nu g/2)$ by $-\cot(\beta_\nu g/2)$ in Eq. (2.10) and $\tan(\beta_\sigma g/2)$ by $-\cot(\beta_\sigma g/2)$ in Eq. (3.6) and repeating the calculation of frequency and polarizability.

The polarizability obtained in this way will be a function of the geometrical parameters $a/b, g/a, a/L, \ell$, and N of the $\mathrm{TM}_{0N\ell}$ cavity mode. In order to tie the polarizability to the geometry of the hole alone, it is necessary to take the limit for large b and L, but with finite frequency. This can be accomplished by letting $b, L\to\infty$, but keeping

$$s \equiv s_N a/b, \quad t \equiv \ell\pi a/L \tag{5.6}$$

finite by also allowing $N, \ell \to \infty$. Obviously

$$k_{N\ell}^2 a^2 = s^2 + t^2 \tag{5.7}$$

and the polarizability of the hole will be a function of $s, t, g/a$. The details are contained in Sec. VII.

VI. GENERALIZED SUSCEPTIBILITY FOR A CIRCULAR HOLE

We now must use the waveguide modes TM_{1n} and TE_{1n} for our complete set. Specifically we have in the pipe region

$$\boldsymbol{e}_n = -\boldsymbol{\nabla}\phi_n,$$

$$\phi_n = \sqrt{\frac{2}{\pi}} \frac{J_1(p_n r/b)\cos\theta}{p_n J_0(p_n)} \quad \text{for } TM_{1n} \text{ modes}, \tag{6.1}$$

$$\boldsymbol{e}_n = \hat{\boldsymbol{z}} \times \boldsymbol{\nabla}\psi_n,$$

$$\psi_n = \sqrt{\frac{2}{\pi}} \frac{J_1(q_n r/b)\sin\theta}{\sqrt{q_n^2 - 1}J_1(q_n)} \quad \text{for } TE_{1n} \text{ modes}, \tag{6.2}$$

and in the iris region

$$\boldsymbol{e}_\nu = -\boldsymbol{\nabla}\phi_\nu,$$

$$\phi_\nu = \sqrt{\frac{2}{\pi}} \frac{J_1(p_\nu r/a)\cos\theta}{p_\nu J_0(p_\nu)} \quad \text{for } TM_{1\nu} \text{ modes}, \tag{6.3}$$

$$\boldsymbol{e}_\nu = \hat{\boldsymbol{z}} \times \boldsymbol{\nabla}\psi_\nu,$$

$$\psi_\nu = \sqrt{\frac{2}{\pi}} \frac{J_1(q_\nu r/a)\sin\theta}{\sqrt{q_\nu^2 - 1}J_1(q_\nu)} \quad \text{for } TE_{1\nu} \text{ modes}, \tag{6.4}$$

where $p_{n,\nu}$ are the roots of $J_1(p_{n,\nu}) = 0$ and $q_{n,\nu}$ are the roots of $J_1'(q_{n,\nu}) = 0$. Once again

$$K_{\sigma\nu}^{\psi} = \delta_{\sigma\nu}, \tag{6.5}$$

but now n and ν can be either TM or TE in $K_{n\nu}^{\psi}$. Again, the superscript ψ denotes susceptibility. Specifically, for n TM and ν TM,

$$K_{n\nu}^{\psi} = -\frac{2a^2 p_n J_1(p_n a/b)}{b^2 J_0(p_n)[p_\nu^2 - (p_n a/b)^2]}; \tag{6.6}$$

for n TM and ν TE,

$$K_{n\nu}^{\psi} = \frac{2J_1(p_n a/b)}{\sqrt{q_\nu^2 - 1}p_n J_0(p_n)}; \tag{6.7}$$

for n TE and ν TM,

$$K_{n\nu}^{\psi} = 0; \tag{6.8}$$

and for n TE and ν TE,

$$K_{n\nu}^{\psi} = \frac{2aq_\nu^2 q_n J_1'(q_n a/b)}{b\sqrt{q_n^2 - 1}\sqrt{q_\nu^2 - 1}J_1(q_n)[q_\nu^2 - (q_n a/b)^2]}. \tag{6.9}$$

The frequency is again obtained from Eq. (3.13) but the symmetric susceptibility requires using Eq. (4.15). Once again the asymmetric susceptibility is obtained by replacing $\tan(\beta_\nu g/2)$ by $-\cot(\beta_\nu g/2)$ in the matrix elements

$$M_{\nu\mu}^{\psi} = \delta_{\nu\mu}\lambda_\nu \tan\frac{\beta_\nu g}{2} - \sum_{n\neq N}{}' \lambda_n \cot\beta_n L \; K_{n\nu}^{\psi} K_{n\mu}^{\psi}. \tag{6.10}$$

In Appendix A we use a different complete set for $\boldsymbol{f}_\nu$, whose first member is the known solution for $\boldsymbol{u}$ in Eqs. (2.4) and (2.9) for a wall of zero thickness. In this way, the variational form allows us to derive the k^2a^2 correction to the polarizability without further analysis. The corresponding result for the susceptibility is obtained in Appendix B. These results are then used in Sec. IX as the framework for displaying the numerical results.

VII. GENERALIZED POLARIZABILITY OF A CIRCULAR HOLE IN A THICK INFINITE PLATE

At the end of Sec. V, we indicated that the polarizability of a circular hole in an infinite plate could be obtained by proceeding to the limit $b, L \to \infty$ with

$$s \equiv s_N a/b, \quad t \equiv \ell\pi a/L, \quad k_{N\ell}^2 a^2 = s^2 + t^2 \tag{7.1}$$

kept finite by letting $N, \ell \to \infty$. We now need the limiting form of Eq. (5.3) for $n \to \infty$, which is obtained by writing

$$|J_1(s_n)| \cong \sqrt{2/\pi s_n}, \tag{7.2}$$

leading to

$$K_{n\nu}^{\chi} \to \sqrt{\frac{2\pi a}{b}} \frac{u^{3/2} J_0(u)}{s_\nu^2 - u^2}, \tag{7.3}$$

with

$$u \equiv s_n a/b. \tag{7.4}$$

We also have

$$\frac{k}{\beta_n} \cot\beta_n L = -\frac{ka \coth\rho_n L}{\rho_n a} \cong -\frac{ka}{\rho_n a}, \tag{7.5}$$

where, as in Eq. (A12),

$$\rho_n a = \sqrt{u^2 - k^2 a^2} \tag{7.6}$$

and $\rho_n L$ is sufficiently large so that $\coth\rho_n L$ can be replaced by 1.

The sum over n in Eq. (5.5) can now be replaced, for large b, by an integral over u, with

$$\sum_n \to \frac{b}{\pi a}\int_0^\infty du. \tag{7.7}$$

Thus we obtain for the matrix element $M_{\nu\mu}^{\chi}$, in the limit of infinite b and L,

$$M_{\nu\mu}^{\chi} \to kaG_{\nu\mu}^{\chi}, \tag{7.8}$$

where

$$G^{\chi}_{\nu\mu} \equiv \frac{\delta_{\nu\mu}}{\beta_\nu a}\tan\frac{\beta_\nu g}{2} + 2m_{\nu\mu}, \tag{7.9}$$

with

$$m_{\nu\mu} \equiv \int_0^\infty \frac{du}{\sqrt{u^2-k^2a^2}}\frac{u^3 J_0^2(u)}{(s_\nu^2-u^2)(s_\mu^2-u^2)} = \frac{1}{s_\mu^2-s_\nu^2}[s_\nu^2 Q(s_\nu) - s_\mu^2 Q(s_\mu)]. \tag{7.10}$$

Here

$$Q(w) \equiv \int_0^\infty \frac{du\; u J_0^2(u)}{\sqrt{u^2-k^2a^2}(w^2-u^2)} \tag{7.11}$$

is a well convergent integral since $J_0(s_\nu)=0$. It should be noted that $Q(w)$ is complex for finite ka, the imaginary part being related to the radiation loss through the hole.

Once $M^{\chi}_{\nu\mu}$ is calculated and we use Eq. (7.3) to write

$$K^{\chi}_{N\nu}K^{\chi}_{N\mu} = \frac{2\pi a}{b}\frac{s^3 J_0^2(s)}{(s_\nu^2-s^2)(s_\mu^2-s^2)}, \tag{7.12}$$

we obtain from Eq. (3.13)

$$\tan\beta_N L = \frac{2\pi}{\beta_N b}s^3 J_0^2(s)\sum_\nu\sum_\mu \frac{1}{s_\nu^2-s^2}(\boldsymbol{G}^{-1})_{\nu\mu}\frac{1}{s_\mu^2-s^2}. \tag{7.13}$$

For large b, L the right-hand side of Eq. (7.12) is small and $\tan\beta_N L$ can be approximated as

$$\tan\beta_N L \cong \beta_N L - \ell\pi \cong \left(\beta_N^2 - \frac{\ell^2\pi^2}{L^2}\right)\frac{L}{2\beta_N} = (k^2-k_{N\ell}^2)\frac{L}{2\beta_N}. \tag{7.14}$$

Using Eqs. (4.14), (A23), and (7.13) for large s_N we obtain

$$\tilde{\chi}_s = \frac{\chi}{4a^3/3} = \frac{(k^2-k_{N\ell}^2)Lb}{4s^3/3} \cong \frac{3\beta_N b}{2s^3}\tan\beta_N L = 3\pi J_0^2(s)\sum_\nu\sum_\mu \frac{1}{s_\nu^2-s^2}(\boldsymbol{G}^{-1})_{\nu\mu}\frac{1}{s_\mu^2-s^2}, \tag{7.15}$$

an expression depending only on $s, k_{N\ell}a$, and g/a or, using Eq. (5.7), on s, t, and g/a. The parameter ka is now replaced by $k_{N\ell}a$ in the last form of Eq. (7.15). Note that $\tilde{\chi}_s$ is the symmetric polarizability in units of that for a small hole in a plate of zero thickness. The corresponding expression for the asymmetric polarizability is obtained by replacing $\tan(\beta_\nu g/2)$ by $-\cot(\beta_\nu g/2)$ in Eq. (7.9).

For $g=0$ and $ka\le 1$, $s\le 1$, the result for $\tilde{\chi}_s$ should approach that in Eq. (A24). We shall see in Sec. IX on numerical results that it does.

VIII. GENERALIZED SUSCEPTIBILITY OF A CIRCULAR HOLE IN A THICK INFINITE PLATE

A calculation similar to that in Sec. VII can be performed for the susceptibility. Setting

$$u = p_n a/b\ ,\ v = q_n a/b, \tag{8.1}$$

we find from Eqs. (6.6)–(6.9), in the limit of small a/b and large n, that for n TM and ν TM,

$$K^{\psi}_{n\nu} \to -\sqrt{\frac{2\pi a}{b}}\frac{u^{3/2}J_1(u)}{p_\nu^2-u^2}; \tag{8.2}$$

for n TM and ν TE,

$$K^{\psi}_{n\nu} \to \sqrt{\frac{2\pi a}{b}}\frac{u^{-1/2}J_1(u)}{\sqrt{q_\nu^2-1}}; \tag{8.3}$$

for n TE and ν TM,

$$K^{\psi}_{n\nu} = 0; \tag{8.4}$$

and for n TE and ν TE,

$$K^{\psi}_{n\nu} \to \sqrt{\frac{2\pi a}{b}}\frac{q_\nu^2}{\sqrt{q_\nu^2-1}}\frac{v^{1/2}J_1'(v)}{q_\nu^2-v^2}. \tag{8.5}$$

From Eq. (6.10) we then find that for μ TM and ν TM (n TM),

$$M^{\psi}_{\nu\mu} = ka\frac{\delta_{\mu\nu}}{\beta_\nu a}\tan\frac{\beta_\nu g}{2} + 2ka\int_0^\infty \frac{u^3 J_1^2(u)du}{(p_\nu^2-u^2)(p_\mu^2-u^2)\sqrt{u^2-k^2a^2}}; \tag{8.6}$$

for μ TM and ν TE (n TM),

$$M^{\psi}_{\nu\mu} = -\frac{2ka}{\sqrt{q_\nu^2-1}}\int_0^\infty \frac{uJ_1^2(u)du}{(p_\mu^2-u^2)\sqrt{u^2-k^2a^2}}; \tag{8.7}$$

and for μ TE and ν TE (n TM and TE),

$$M^{\psi}_{\nu\mu} = \frac{\delta_{\nu\mu}\beta_\nu a}{ka}\tan\frac{\beta_\nu g}{2} + \frac{2ka}{\sqrt{(q_\nu^2-1)(q_\mu^2-1)}}\left[\int_0^\infty \frac{J_1^2(u)du}{u\sqrt{u^2-k^2a^2}} - \frac{q_\nu^2 q_\mu^2}{k^2a^2}\int_0^\infty \frac{[J_1'(v)]^2 v\sqrt{v^2-k^2a^2}dv}{(q_\nu^2-v^2)(q_\mu^2-v^2)}\right]. \tag{8.8}$$

These matrix elements can be written in terms of integrals similar to the $Q(w)$, defined in Eq. (7.11). Specifically, for μ TM and ν TM (n TM),

$$M^{\psi}_{\nu\mu} = ka\left[\frac{\delta_{\mu\nu}}{\beta_\nu a}\tan\frac{\beta_\nu g}{2} + \frac{2}{p_\mu^2-p_\nu^2}[p_\nu^2 R(p_\nu) - p_\mu^2 R(p_\mu)]\right]; \tag{8.9}$$

for μ TM and ν TE (n TM),

$$M^{\psi}_{\nu\mu} = -\frac{2ka}{\sqrt{q_\nu^2 - 1}} R(p_\mu); \tag{8.10}$$

and for μ TE and ν TE (n TM and TE),

$$M^{\psi}_{\nu\mu} = \delta_{\mu\nu} \frac{\beta_\nu a}{ka} \tan \frac{\beta_\nu g}{2} - \frac{2ka}{\sqrt{(q_\nu^2 - 1)(q_\mu^2 - 1)}} R(0) + \frac{2q_\mu^2 q_\nu^2}{ka\sqrt{(q_\nu^2 - 1)(q_\mu^2 - 1)}} \frac{S(q_\nu) - S(q_\mu)}{q_\nu^2 - q_\mu^2}, \tag{8.11}$$

where

$$R(w) = \int_0^\infty \frac{du\ u\ J_1^2(u)}{(w^2 - u^2)\sqrt{u^2 - k^2a^2}}, \tag{8.12}$$

$$S(w) = \int_0^{ka} \frac{du\ u\ [J_1'(u)]^2 \sqrt{u^2 - k^2a^2}}{w^2 - u^2} + w^2 \int_{ka}^\infty \frac{du}{u} \frac{[J_1'(u)]^2 \sqrt{u^2 - k^2a^2}}{(w^2 - u^2)}. \tag{8.13}$$

Once $M^{\psi}_{\nu\mu}$ is calculated, we use

$$p \equiv p_N a/b\ ,\ q \equiv q_N a/b, \tag{8.14}$$

as in Eq. (B35), to write for μ TM, ν TM, and N TM,

$$K^{\psi}_{N\nu} K^{\psi}_{N\mu} = \frac{2\pi a}{b} \frac{p^3 J_1^2(p)}{(p_\nu^2 - p^2)(p_\mu^2 - p^2)}; \tag{8.15}$$

for μ TM, ν TM, and N TE,

$$K^{\psi}_{N\nu} K^{\psi}_{N\mu} = 0; \tag{8.16}$$

for μ TM, ν TE, and N TM,

$$K^{\psi}_{N\nu} K^{\psi}_{N\mu} = -\frac{2\pi a}{b} \frac{p J_1^2(p)}{\sqrt{q_\nu^2 - 1}(p_\nu^2 - p^2)}; \tag{8.17}$$

for μ TM, ν TE, and N TE,

$$K^{\psi}_{N\nu} K^{\psi}_{N\mu} = 0; \tag{8.18}$$

for μ TE, ν TE, and N TM,

$$K^{\psi}_{N\nu} K^{\psi}_{N\mu} = \frac{2\pi a}{b} \frac{J_1^2(p)}{p\sqrt{(q_\nu^2 - 1)(q_\mu^2 - 1)}}; \tag{8.19}$$

and for μ TE, ν TE, and N TE,

$$K^{\psi}_{N\nu} K^{\psi}_{N\mu} = \frac{2\pi a}{b} \frac{q_\mu^2 q_\nu^2}{\sqrt{(q_\nu^2 - 1)(q_\mu^2 - 1)}} \frac{q[J_1'(q)]^2}{(q_\nu^2 - q^2)(q_\mu^2 - q^2)}. \tag{8.20}$$

Finally, we obtain the renormalized symmetric susceptibility as

$$\tilde{\psi}_s = \frac{\psi}{8a^3/3} = -\frac{3\pi}{ka} \sum_\mu \sum_\nu K^{\psi}_{N\nu} K^{\psi}_{N\mu} (M^{-1})_{\mu\nu}, \tag{8.21}$$

where the μ and ν extend over both TE and TM modes in the matrix $\boldsymbol{M}$ and its inverse. The asymmetric susceptibility is obtained by replacing $\tan(\beta_\nu g/2)$ by $-\cot(\beta_\nu g/2)$ in Eqs. (8.6), (8.8), (8.9), and (8.11).

For $g = 0$ and small ka,p,q, the results for $\tilde{\psi}_s$ should reduce to those in Eqs. (B33) and (B34). We shall see in the following section on numerical results that they do.

IX. NUMERICAL RESULTS FOR A HOLE IN A PLATE

We have analyzed the generalized polarizability of a circular hole in a thick plate and found that it depends on the geometry of the hole (g/a) and, as expected, on ka, the ratio of the hole radius to the reduced wavelength $\lambda/2\pi$. What may not have been expected is the dependence on s.

This represents the fact that higher-order terms involve separately the dependence of the electric field on r and z near the hole. Specifically

$$s^2 = a^2 \nabla_\perp^2 E_z / E_z(0) \tag{9.1}$$

while

$$k^2a^2 - s^2 = a^2 \frac{\partial^2 E_z}{\partial z^2} / E_z(0). \tag{9.2}$$

All numerical results for the polarizability of a circular hole in a thick plate were obtained using Eq. (7.15) for various values of ka, s, and g/a. In this process the integral for $Q(w)$ in Eq. (7.15) was evaluated numerically for various values of ka and $w = s_\nu$ and the matrix $\boldsymbol{G}$ was truncated at an order sufficient to achieve the desired accuracy. We note that $Q(w)$ also has an imaginary part, leading to a small imaginary contribution to the polarizability for small ka.

We present the results in a form suggested by the predictions for $g = 0$ and small ka,s in Eq. (A24). Specifically, we have for the real part of the symmetric polarizability

$$\tilde{\chi}_s(ka, s) \equiv \chi/(4a^3/3) \cong 1 - \frac{k^2a^2}{5} - \frac{s^2}{5} \tag{9.3}$$

and plot $\tilde{\chi}_s$ vs s^2 for various values of ka in Fig. 2. We

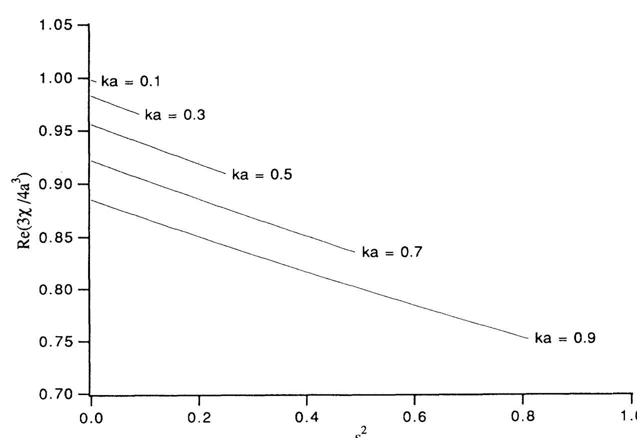

FIG. 2. Real part of the scaled polarizability $\tilde{\chi}_s$ vs s^2 for various ka, with $g/a = 0$.

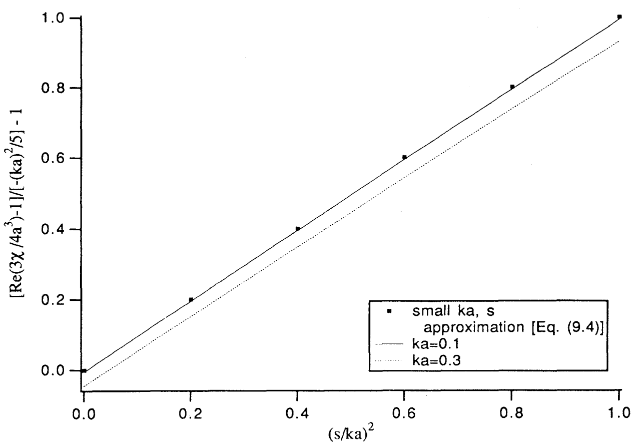

FIG. 3. Real part of the scaled polarizability $\hat{\chi}_s$ vs $(s/ka)^2$ for $ka = 0.1$ and 0.3, with $g/a = 0$.

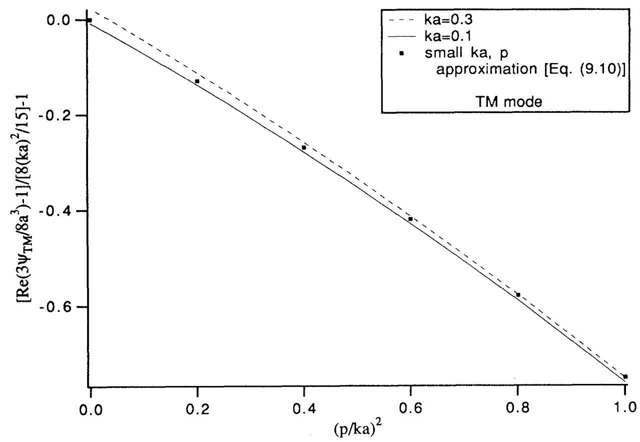

FIG. 5. Real part of the scaled susceptibility $\hat{\psi}_s$ vs $(p/ka)^2$ (for the TM mode) for $ka = 0.1$ and 0.3, with $g/a = 0$.

define $\hat{\chi}$ as

$$\hat{\chi} = \frac{\tilde{\chi}(ka, s) - \tilde{\chi}(0,0)}{(-k^2a^2/5)} - 1 \cong \frac{s^2}{k^2a^2} \tag{9.4}$$

and plot $\hat{\chi}$ vs s^2/k^2a^2 for various values of ka in Fig. 3. Note that $k^2a^2 = s^2 + (\ell\pi a/L)^2$, so that s^2/k^2a^2 is always between 0 and 1.

A similar presentation is provided for the real part of the scaled susceptibilities in Figs. 4–6. Once again we have an additional dependence on the transverse second derivatives for both the TM and the TE mode in the form

$$p^2 = a^2 \nabla_\perp^2 H_y / H_y(0) \quad \text{(TM)}, \tag{9.5}$$

$$q^2 = a^2 \nabla_\perp^2 H_y / H_y(0) \quad \text{(TE)}. \tag{9.6}$$

The fact that the TM and TE modes give different results when the cavity walls are moved to infinity is at first surprising, since TM and TE refer to the boundary conditions at infinity. But the problem no longer has azimuthal symmetry within the hole and we must allow $\partial^2 H_y/\partial x^2$ and $\partial^2 H_y/\partial y^2$ to be different in general for a hole. This issue is discussed in greater depth in Appendix B following Eq. (B35).

We now define $\tilde{\psi}$ as

$$\tilde{\psi} = \psi/(8a^3/3) \tag{9.7}$$

and are guided by the $g = 0$, small ka,p,q results in Eqs. (B33) and (B34), which are

$$\tilde{\psi}_{\rm TM} \cong 1 + k^2a^2 \left(\frac{8}{15} - \frac{p^2}{3k^2a^2} - \frac{p^4}{15k^4a^4} \right) \tag{9.8}$$

and

$$\tilde{\psi}_{\rm TE} \cong 1 + k^2a^2 \left(\frac{8}{15} - \frac{q^2}{5k^2a^2} \right). \tag{9.9}$$

In particular, we define $\hat{\psi}$ as

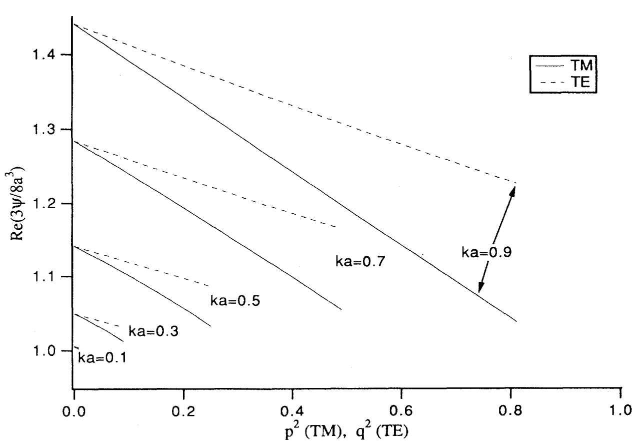

FIG. 4. Real part of the scaled susceptibility $\tilde{\psi}_s$ vs p^2 (for the TM mode) and q^2 (for the TE mode) for various ka, with $g/a = 0$.

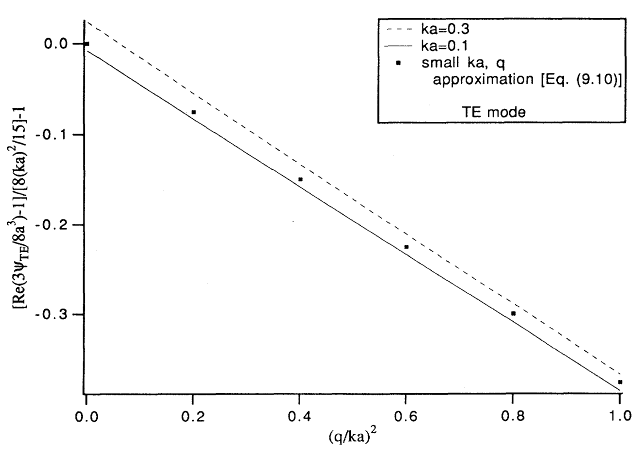

FIG. 6. Real part of the scaled susceptibility $\hat{\psi}_s$ vs $(q/ka)^2$ (for the TE mode) for $ka = 0.1$ and 0.3, with $g/a = 0$.

$$\hat{\psi} = \frac{\tilde{\psi}(ka, p, \text{ or } q) - \tilde{\psi}(0,0)}{(8k^2a^2/15)} - 1$$

$$= -\begin{cases} \frac{5p^2}{8k^2a^2} + \frac{p^4}{8k^4a^4}, & \text{TM} \\ \frac{3q^2}{8k^2a^2}, & \text{TE} \end{cases} \quad (9.10)$$

and plot $\hat{\psi}$ vs p^2/k^2a^2 (TM) or q^2/k^2a^2 (TE) for various values of ka. Once again p^2/k^2a^2 and q^2/k^2a^2 are between 0 and 1.

Figures 2–6 for $g = 0$ and reasonably small ka show clearly the validity of the approximation in Eqs. (9.4) and (9.10), including the quadratic variation for the real part of the symmetric TM susceptibility. The numerical coefficients in these equations are very similar to those derived by Eggimann [9], who studied diffraction by a circular disk. He used a power series expansion to obtain the frequency dependence of the dipole moments, but apparently did not include higher multipole moments in his final results. It is also possible that our cavity problem may not be identical to the diffraction problem studied by Eggimann.

The numerical coefficient for $s = ka$ in the polarizability also agrees with the value quoted by Sporleder and Unger [10], but the coefficients in the susceptibility for $p = q = ka$ are different from those quoted by these authors.

As stated before, the integrals $Q(w)$ in Eq. (7.11) and $S(w)$ in Eq. (8.13) contribute an imaginary part to the generalized polarizability and susceptibilities, respectively. These imaginary parts correspond to radiation loss through the hole. The dependence of Im$\tilde{\chi}$ vs s^2 and Im$\tilde{\psi}$ vs p^2,q^2 is shown in Figs. 7 and 8 for various values of ka.

Our analytic approximate formulas for polarizability and susceptibility should be modified to include these imaginary parts. For small ka the left-hand side of Eq. (A18) contains an imaginary contribution from $x = 0$ to $x = ka$. This eventually leads to a modification of Eq. (A24) according to

$$\chi_{N\ell} \cong \frac{4a^3}{3}\left(1 - \frac{k^2a^2}{5} - \frac{s^2}{5} + \frac{4j}{9\pi}k^3a^3\right). \quad (9.11)$$

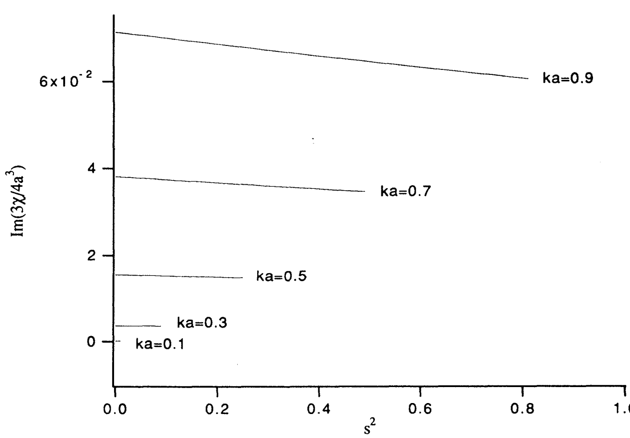

FIG. 7. Imaginary part of the scaled polarizability $\tilde{\chi}_s$ vs s^2 for various ka, with $g/a = 0$.

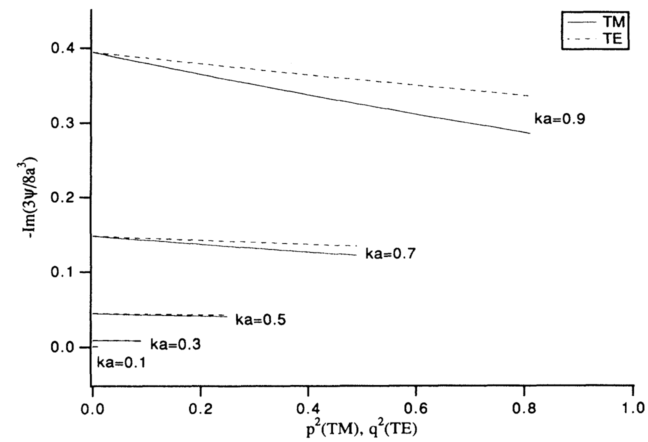

FIG. 8. Imaginary part of the scaled susceptibility $\tilde{\psi}_s$ vs p^2 (for the TM mode) and q^2 (for the TE mode) for various ka, with $g/a = 0$.

Similarly, we obtain a comparable imaginary part from both terms in the first version of Eq. (B18) in the range from $x = 0$ to $x = ka$, which adds a small imaginary part to Eqs. (B33) and (B34) in the form

$$\psi_{N\ell} \cong \frac{8a^3}{3}\left[1 + k^2a^2\left(\frac{8}{15} - \frac{p^2}{3k^2a^2} - \frac{p^4}{15k^4a^4}\right) - \frac{8j}{9\pi}k^3a^3\right] \quad \text{(TM)}, \quad (9.12)$$

$$\psi_{N\ell} \cong \frac{8a^3}{3}\left[1 + k^2a^2\left(\frac{8}{15} - \frac{q^2}{5k^2a^2}\right) - \frac{8j}{9\pi}k^3a^3\right] \quad \text{(TE)}. \quad (9.13)$$

The leading imaginary term in Eqs. (9.11)–(9.13) for $g = 0$ and small ka appears to be well confirmed. Moreover, these terms are the same as those obtained by Eggimann [9].

For the wall with finite thickness, the polarizability and susceptibility seen within the cavity are given by [6]

$$\chi_{\text{in}} = \chi_s + \chi_a, \quad \psi_{\text{in}} = \psi_s + \psi_a, \quad (9.14)$$

while the polarizability and susceptibility seen outside the cavity are given by

$$\chi_{\text{out}} = \chi_s - \chi_a, \quad \psi_{\text{out}} = \psi_s - \psi_a. \quad (9.15)$$

Here the subscripts s and a denote the solutions of the symmetric and antisymmetric potential problems [6]. In Figs. 9 and 10 we show $\tilde{\chi}_{\text{in}}$ and $\tilde{\psi}_{\text{in}}$ as functions of g/a for various ka. Figures 11 and 12 show the dependence of ln$\tilde{\chi}_{\text{out}}$ and ln$\tilde{\psi}_{\text{out}}$ on g/a. In the limit of $ka = 0$, our results are in agreement with those given in Ref. [4] to four significant figures. As $g/a \to 0$, the zero thickness results are recovered: $\chi_{\text{in}} = \chi_{\text{out}} \to 4a^3/3$, $\psi_{\text{in}} = \psi_{\text{out}} \to 8a^3/3$. And as g/a becomes large, the logarithmic plots of $\tilde{\chi}_{\text{out}}$ and $\tilde{\psi}_{\text{out}}$ become linear with slopes $-s_1 = -2.405$ and $-q_1 = -1.841$, respectively. The fact that slopes

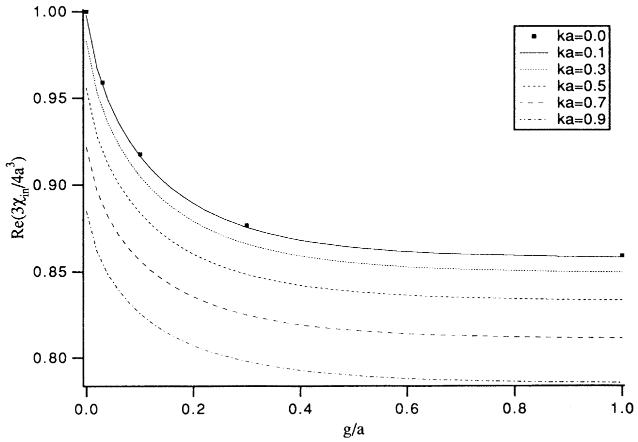

FIG. 9. Real part of the scaled polarizability $\tilde{\chi}_{\rm in}$ vs g/a for various ka, with $s = 0$.

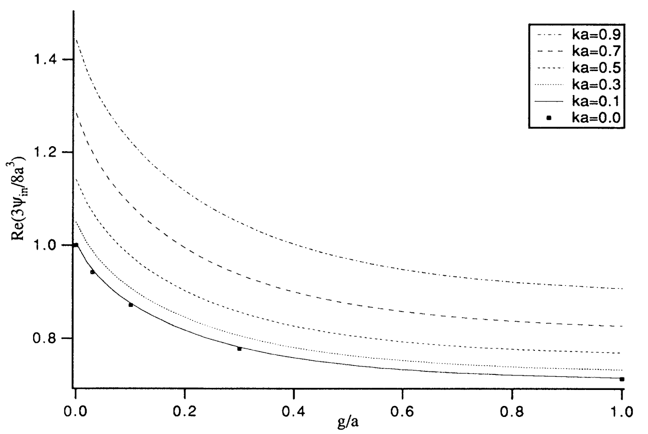

FIG. 10. Real part of the scaled susceptibility $\tilde{\psi}_{\rm in}$ vs g/a for various ka, with $p = 0$ (for the TM mode) or $q = 0$ (for the TE mode), where the curves are the same for both TM and TE modes.

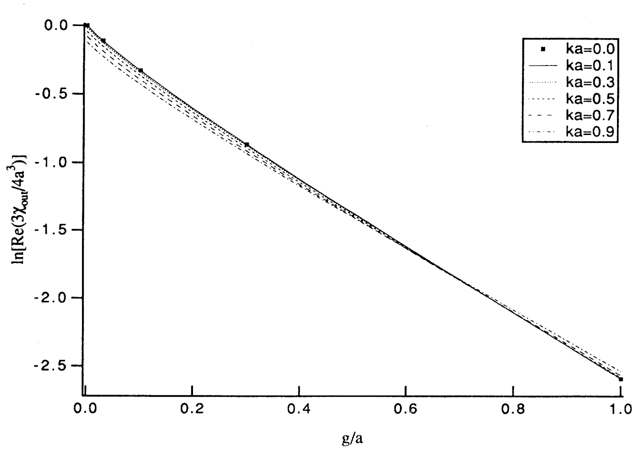

FIG. 11. Natural logarithm of the real part of the scaled polarizability $\tilde{\chi}_{\rm out}$ vs g/a for various ka, with $s = 0$.

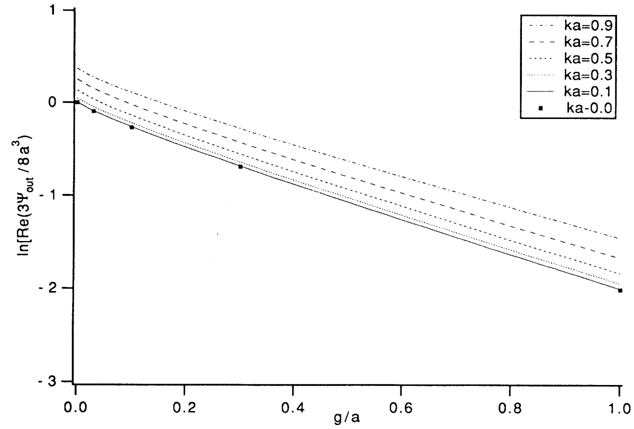

FIG. 12. Natural logarithm of the real part of the scaled susceptibility $\tilde{\psi}_{\rm out}$ vs g/a for various ka, with $p = 0$ (for the TM mode) or $q = 0$ (for the TE mode), where the curves are the same for both TM and TE modes.

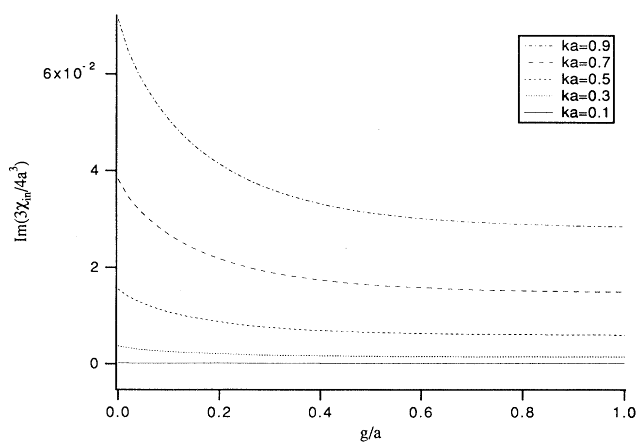

FIG. 13. Imaginary part of the scaled polarizability $\tilde{\chi}_{\rm in}$ vs g/a for various ka, with $s = 0$.

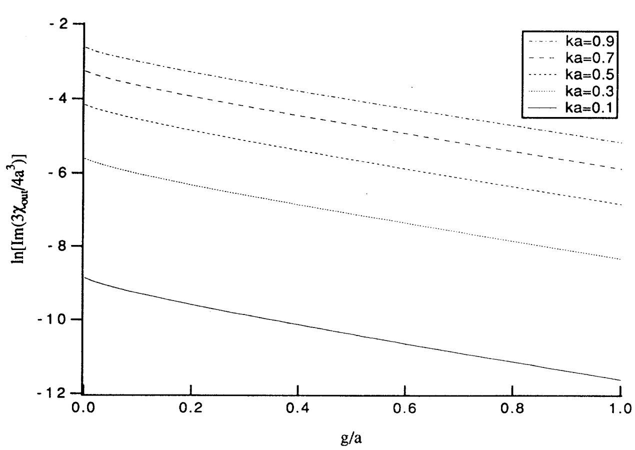

FIG. 14. Natural logarithm of the imaginary part of the scaled polarizability $\tilde{\chi}_{\rm out}$ vs g/a for various ka, with $s = 0$.

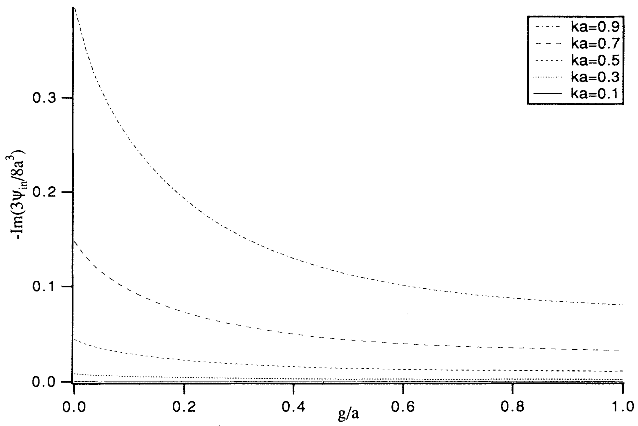

FIG. 15. Imaginary part of the scaled susceptibility $\tilde{\psi}_{\rm in}$ vs g/a for various ka, with $p = 0$ (for the TM mode) or $q = 0$ (for the TE mode), where the curves are the same for both TM and TE modes.

are equal to the first zeros of $J_0(s)$ and $J_1'(q)$ reflects the dominance of the lowest modes, i.e., the modes with the smallest exponential dropoff along the z axis, for the thick wall. The small change of the asymptotic slopes of the curves in Figs. 11, 12, 14, and 16 for different ka shows that the lowest modes are still dominant, even for finite ka. In Figs. 13–16 we show the imaginary parts of $\tilde{\chi}_{\rm in}$, $\ln\tilde{\chi}_{\rm out}$, $\tilde{\psi}_{\rm in}$, and $\ln\tilde{\psi}_{\rm out}$ vs g/a for various ka.

X. DISCUSSION AND SUMMARY

We have defined a generalized polarizability and susceptibility of a hole for finite wavelength in terms of the frequency shift of the associated cavities due to the hole. In addition, we have constructed a variational form for these frequency shifts, thus ensuring good convergence for our numerical calculations. We then allow the cavity dimensions to be infinitely large, enabling us to obtain the generalized polarizability and susceptibilities of a circular hole in an infinite plate of finite thickness. Then, we obtain numerical results for various values of $ka,g/a,s,p,q$ and note that there are in general two distinct values of the susceptibility depending on the second derivative of the magnetic field in and perpendicular to the direction of the original magnetic field at the hole location.

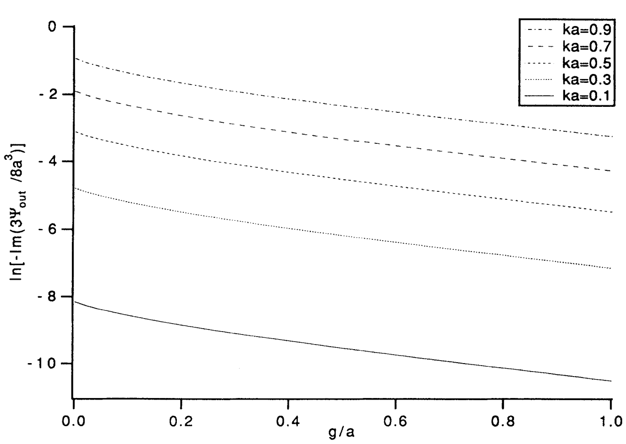

FIG. 16. Natural logarithm of the imaginary part of scaled susceptibility $\tilde{\psi}_{\rm out}$ vs g/a for various ka, with $p = 0$ (for the TM mode) or $q = 0$ (for the TE mode), where the curves are the same for both TM and TE modes.

The variational formulation also allows us to obtain first-order corrections in k^2a^2, s^2, p^2, and q^2 analytically for a hole in a plate of zero thickness. Here s^2, p^2, and q^2 describe the transverse dependence of the fields without the hole and these are needed because the corrections will depend separately on the behavior of the fields in the longitudinal and transverse directions.

The approximate forms obtained with the first-order corrections have been compared with our numerical results and appear to be valid for ka as large as 1, with $s \leq ka$, $p \leq ka$, and $q \leq ka$. These forms are very similar to those obtained by others for diffraction of a plane wave through a hole in a metallic plate or by a metallic disk. Although the numerical procedures allow us to consider much higher values of ka, the results will be extremely complicated since there will be propagation through the iris holes and one can expect resonant coupling. This has not been studied in the present paper.

ACKNOWLEDGMENTS

The authors wish to thank Dr. N.I. Aizatsky for several helpful comments. This work was supported by the U.S. Department of Energy.

APPENDIX A: ALTERNATE BASIS FUNCTIONS FOR THE GENERALIZED POLARIZABILITY—ANALYTIC APPROXIMATION FOR A SMALL HOLE IN A THIN WALL

It is well known [1] that for a wall of zero thickness, the function $\boldsymbol{u}(\boldsymbol{r})$ for the polarizability calculation is

$$\boldsymbol{u}(\boldsymbol{r}) = -\boldsymbol{\nabla}\left(1-\frac{r^2}{a^2}\right)^{1/2} \tag{A1}$$

for a circular hole whose radius is much smaller than the wavelength. When calculating the polarizability, we therefore may wish to use the set of functions

$$\boldsymbol{f}_\nu(\boldsymbol{r}) = -\boldsymbol{\nabla}\left(1-\frac{r^2}{a^2}\right)^{\nu-1/2} \tag{A2}$$

in Eq. (3.4), where $\nu = 1,2,3,\ldots$. In order to evaluate the integrals in Eq. (3.7) we use

$$\begin{aligned} 2\pi\int_0^a r dr \boldsymbol{\nabla}\left(1-\frac{r^2}{a^2}\right)^{\nu-1/2} \cdot \boldsymbol{\nabla} J_0(\kappa r) &= 2\pi\kappa^2\int_0^a r dr\left(1-\frac{r^2}{a^2}\right)^{\nu-1/2} J_0(\kappa r) \\ &= \pi\kappa^2 a^2 G_\nu(\kappa a), \end{aligned} \tag{A3}$$

with $\kappa = s_n/b$. The function $G_\nu(w)$ is defined as

$$G_\nu(w) \equiv \Gamma\left(\nu + \frac{1}{2}\right) \frac{J_{\nu+1/2}(w)}{(w/2)^{\nu+1/2}} = \frac{\Gamma(\nu+1/2)}{\Gamma(3/2)} \frac{j_\nu(w)}{(w/2)^\nu}, \quad (A4)$$

where $j_\nu(w)$ is the spherical Bessel function of order ν. This expression can be obtained by expanding $J_0(\kappa r)$ into a power series in $\kappa^2 r^2$ and integrating term by term in Eq. (A3). We then have

$$K^\chi_{n\nu} = \sqrt{\pi}\frac{a^2}{b^2}\frac{s_n}{J_1(s_n)} G_\nu\left(\frac{s_n a}{b}\right),$$

$$K^\chi_{\sigma\nu} = \sqrt{\pi}\frac{s_\sigma}{J_1(s_\sigma)} G_\nu(s_\sigma). \quad (A5)$$

The matrix in Eq. (3.6) then becomes

$$M^\chi_{\nu\mu} = -\sum_{n\neq N}{}' \frac{k}{\beta_n} \cot\beta_n L\, K^\chi_{n\nu} K^\chi_{n\mu} + \sum_\sigma \frac{k}{\beta_\sigma} \tan\frac{\beta_\sigma g}{2} K^\chi_{\sigma\nu} K^\chi_{\sigma\mu}. \quad (A6)$$

We now consider only the case $g = 0$, separate out the $\nu = 1$, $\mu = 1$ term, and write $d_\nu = c_\nu/c_1$ in Eq. (3.5) to obtain

$$\frac{k\cot\beta_N L}{\beta_N} = \frac{M^\chi_{11} + 2\sum_{\nu=2}^\infty d_\nu M^\chi_{1\nu} + \sum_{\nu=2}^\infty\sum_{\mu=2}^\infty d_\nu d_\mu M^\chi_{\nu\mu}}{\left(K^\chi_{N1} + \sum_{\nu=2}^\infty d_\nu K^\chi_{N\nu}\right)^2}. \quad (A7)$$

Since the $\nu = 1$ term in Eq. (A2) is the correct solution for a small hole with $g = 0$, each d_ν for $\nu \geq 2$ must be proportional to a^2. Expanding the right-hand side of Eq. (A7) in powers of a^2 leads to the form

$$\frac{\cot\beta_N L}{\beta_N} = \frac{M^\chi_{11}}{k(K^\chi_{N1})^2} \times \left[1 + 2\sum_{\nu=2}^\infty d_\nu A_\nu + \sum_{\nu=2}^\infty\sum_{\mu=2}^\infty d_\nu d_\mu B_{\nu\mu}\right], \quad (A8)$$

where A_ν and $B_{\nu\mu}$ are expected to be of order 1. But the minimum value of Eq. (A8) must occur for d_ν proportional to a^2 and this can happen only if A_ν is proportional to a^2. In this case the term in square brackets in Eq. (A8) will be of order $1 + O(a^4)$. The a^2 correction to the static result can therefore be obtained by carrying out the calculation of $M^\chi_{11}/(K^\chi_{N1})^2$ so as to include effects proportional to a^2 and neglecting term of order a^3 or higher. This is equivalent to setting $d_{\nu,\mu} = 0$ in Eq. (A8). Thus we obtain

$$\beta_N \tan\beta_N L \cong \frac{(K^\chi_{N1})^2}{M^\chi_{11}/k}. \quad (A9)$$

From Eq. (A5) we find

$$K^\chi_{n1} = \frac{2\sqrt{\pi}a}{b}\frac{j_1(s_n a/b)}{J_1(s_n)} \quad (A10)$$

and from Eq. (A6)

$$\frac{M^\chi_{11}}{k} = -\sum_{n\neq N}{}' \frac{\cot\beta_n L}{\beta_n}(K^\chi_{n1})^2 = \sum_{n\neq N}{}' \frac{\coth\rho_n L}{\rho_n}(K^\chi_{n1})^2, \quad (A11)$$

where

$$\rho_n \equiv \sqrt{s_n^2/b^2 - k^2}. \quad (A12)$$

Thus we find

$$\beta_N \tan\beta_N L \cong \frac{j_1^2(s_N a/b)}{J_1^2(s_N)} \Bigg/ \sum_{n\neq N}{}' \frac{\coth\rho_n L}{\rho_n}\frac{j_1^2(s_n a/b)}{J_1^2(s_n)}. \quad (A13)$$

If we proceed to the limit $a \to 0$ in Eq. (A13) the primary contributions come from large n and the sum in the denominator goes as $\sum_n n^2$, requiring the use of a cutoff of order $n_{\max} \sim b/a$. In this way we are led to a polarizability of order a^3, as expected. We therefore can evalulate Eq. (A13) by taking the large n limit, using

$$J_1^2(s_n) \cong (2/\pi s_n), \ \coth\rho_n L \cong 1 \quad (A14)$$

and converting the sum over n to an integral over $x = s_n a/b$. Thus

$$\sum_{n\neq N}{}' \to \frac{b^2}{2a}\int_0^\infty \frac{x dx j_1^2(x)}{\sqrt{x^2 - k^2a^2}}. \quad (A15)$$

Since

$$j_1(x) = \left(\frac{\sin x}{x^2} - \frac{\cos x}{x}\right), \quad (A16)$$

we find, up to terms of order a^2/b^2,

$$\beta_N \tan\beta_N L = \frac{2s_N^2 a^3(1 - s_N^2 a^2/5b^2)}{9b^4 J_1^2(s_N) I}, \quad (A17)$$

where

$$I = \int_0^\infty \frac{x dx j_1^2(x)}{\sqrt{x^2 - k^2a^2}} \cong \int_0^\infty dx j_1^2(x) + \frac{k^2a^2}{2}\int_0^\infty \frac{dx j_1^2(x)}{x^2}. \quad (A18)$$

Using $j_1(x)$ in Eq. (A16) and integrating terms successively by parts in Eq. (A18), we find

$$I \cong \frac{\pi}{6}\left(1 + \frac{k^2a^2}{5}\right). \quad (A19)$$

We now consider the cavity mode $\mathrm{TM}_{0N\ell}$, with

$$k^2_{N\ell} = \frac{s_N^2}{b^2} + \frac{\ell^2\pi^2}{L^2}. \quad (A20)$$

Since $\beta_N L$ is now near $\ell\pi$, Eq. (A17) leads to

$$\beta_N \tan\beta_N L \cong \frac{\beta_N(\beta_N^2 L^2 - \ell^2\pi^2)}{\beta_N L + \ell\pi} \cong \frac{4s_N^2 a^3}{3\pi b^4 J_1^2(s_N)}\left(1 - \frac{s_N^2 a^2}{5b^2} - \frac{k_{N\ell}^2 a^2}{5}\right). \tag{A21}$$

Since $\beta_N L - \ell\pi$ is of order a^3, we can set the factor $\beta_N/(\beta_N L + \ell\pi) = 1/2L$, accurate to order a^2. In this way we find

$$k^2 - k_{N\ell}^2 = \frac{\beta_N^2 L^2 - \ell^2\pi^2}{L^2} \cong \frac{8}{3\pi}\frac{s_N^2 a^3}{Lb^4 J_1^2(s_N)}\left(1 - \frac{\ell^2\pi^2 a^2}{5L^2} - \frac{2s_N^2 a^2}{5b^2}\right). \tag{A22}$$

Finally, we can show that for the $\mathrm{TM}_{0N\ell}$ mode

$$k_{N\ell}^2 E_{N\ell}^2(0) = \frac{2s_N^2}{\pi L b^4 J_1^2(s_N)} \tag{A23}$$

and therefore, from Eq. (4.14), we find [7]

$$\chi \cong \frac{k^2 - k_{N\ell}^2}{k_{N\ell}^2 E_{N\ell}^2(0)} \cong \frac{4a^3}{3}\left(1 - \frac{k^2a^2}{5} - \frac{s^2}{5}\right), \tag{A24}$$

where $s \equiv s_N a/b$. Direct numerical evaluation of the sum in Eq. (A13) confirms the fact that there is no a^2/b^2 correction when the sum over n is converted to an integral.

A logical generalization of Eq. (A24) is that, for small a and $g = 0$, the polarizability is of the form

$$\chi \cong \frac{4a^3}{3}\left[1 - \frac{k^2a^2}{5} + \frac{a^2}{5E_z(0)}\nabla_\perp^2 E_z\right], \tag{A25}$$

depending on the second derivatives of the normal electric field component at the center of the hole. We have suppressed the subscripts on k in the correction term in Eqs. (A24) and (A25).

APPENDIX B: GENERALIZED SUSCEPTIBILITY—ANALYTIC APPROXIMATION FOR A SMALL HOLE IN A THIN WALL

For zero wall thickness, the longitudinal component of the magnetic field $H_z(r)$ is proportional to [1]

$$H_z(r,\theta) \to \frac{r\sin\theta}{(1 - r^2/a^2)^{1/2}} = \frac{y}{(1 - r^2/a^2)^{1/2}}. \tag{B1}$$

Unfortunately, the general variational formulation in Sec. III requires that we use trial functions for the transverse *electric* field in the hole, as in Eq. (3.4). We therefore must determine the form of $\boldsymbol{u}(\boldsymbol{r})$ that corresponds to Eq. (B1).

Since $H_z(x, y)$ is proportional to $\partial E_y/\partial x - \partial E_x/\partial y$, we can produce the correct form of H_z for $k \to 0$ by using

$$f_{1x} = (1 - r^2/a^2)^{1/2} - \partial\phi/\partial x, \tag{B2}$$

$$f_{1y} = -\partial\phi/\partial y \tag{B3}$$

in Eq. (3.7). The term in ϕ corresponds to an additional TM component that does not contribute to H_z. At this point our choice of the function ϕ is not obvious, but we should have $\phi(r = a) = 0$ to satisfy the boundary condition on E_θ on the iris wall.

The other members of the set of trial functions for which Eqs. (B2) and (B3) are the first are not obvious. But an argument parallel to the one used in Eqs. (A7)–(A9) permits us to calculate the susceptibility, including corrections of order a^2/b^2 and k^2a^2, from

$$\lambda_N \cot\beta_N L = \frac{M_{11}^\psi}{(K_{N1}^\psi)^2}, \tag{B4}$$

using only the first member of the set. Thus

$$\beta_N \tan\beta_N L = \frac{k(K_{N1}^\psi)^2}{M_{11}^\psi}, \ \mathrm{TM}_{1N\ell} \text{ mode}, \tag{B5}$$

$$\frac{\tan\beta_N L}{\beta_N} = \frac{(K_{N1}^\psi)^2}{kM_{11}^\psi}, \ \mathrm{TE}_{1N\ell} \text{ mode}. \tag{B6}$$

For $g = 0$, the matrix element M_{11}^ψ in Eq. (3.6) is

$$M_{11}^\psi = -{\sum_{n\neq N}}' \lambda_n \cot\beta_n L\,(K_{n1}^\psi)^2, \tag{B7}$$

where the sum over n involves both TE and TM modes, with K_{n1} defined in Eq. (3.7). For n being a TM mode, we can write

$$K_{n1}^\psi = \int_{S_1} dS\ \vec{e}_n\cdot\vec{f}_1 = -\int_{S_1} dS\left(1 - \frac{r^2}{a^2}\right)^{1/2}\frac{\partial\phi_n}{\partial x} + \int_{S_1} dS\ \nabla\phi_n\cdot\nabla\phi = -\int_{S_1} dS\ \phi_n\frac{x}{a^2}\left(1 - \frac{r^2}{a^2}\right)^{-1/2} + \frac{p_n^2}{b^2}\int_{S_1} dS\ \phi_n\phi, \tag{B8}$$

where the final form is a result of integration by parts in each term. Using Eq. (6.1) we find for the first term

$$-\sqrt{\frac{2}{\pi}}\frac{1}{p_n J_0(p_n)}\int_0^{2\pi} d\theta\ \cos^2\theta \times\int_0^a \frac{r^2 dr}{a^2}J_1\left(\frac{p_n r}{b}\right)\left(1 - \frac{r^2}{a^2}\right)^{-1/2}$$
$$= \frac{\sqrt{2\pi}}{p_n J_0(p_n)}\int_0^a r\,dr J_1\left(\frac{p_n r}{b}\right)\frac{\partial}{\partial r}\left(1 - \frac{r^2}{a^2}\right)^{1/2} = -\frac{\sqrt{2\pi}}{bJ_0(p_n)}\int_0^a r\,dr J_0\left(\frac{p_n r}{b}\right)\left(1 - \frac{r^2}{a^2}\right)^{1/2}, \tag{B9}$$

where we have again integrated by parts. Using Eqs. (A3) and (A4) for $\nu = 1$, we therefore have

$$K_{n1}^\psi = -\frac{a^2\sqrt{2\pi}}{bJ_0(p_n)}\frac{j_1(x_n)}{x_n} + \frac{p_n^2}{b^2}\int dS\ \phi_n\phi, \tag{B10}$$

with $x_n = p_n a/b$.

At this point we use the symmetry of the problem and the known behavior of electric fields in the vicinity of a circular hole in a thin wall to try

$$\phi(x,y) = \alpha x(1-r^2/a^2)^{1/2}, \tag{B11}$$

where α is a constant to be determined in the minimization process. An analysis parallel to the preceding one leads to

$$K^{\psi}_{n1} = -\frac{a^2\sqrt{2\pi}}{bJ_0(p_n)}\left[\frac{j_1(x_n)}{x_n} - \alpha j_2(x_n)\right] \quad \text{(TM)}. \tag{B12}$$

If n corresponds to a TE mode, we have

$$\begin{aligned} K^{\psi}_{n1} &= \int_{S_1} dS\, \hat{z}\times\nabla\psi_n\cdot\vec{f}_1 \\ &= -\int_{S_1} dS\, \frac{\partial\psi_n}{\partial y}\left(1-\frac{r^2}{a^2}\right)^{1/2} \\ &\quad -\int_{S_1} dS\left(\frac{\partial\psi_n}{\partial x}\frac{\partial\phi}{\partial y} - \frac{\partial\psi_n}{\partial y}\frac{\partial\phi}{\partial x}\right). \end{aligned} \tag{B13}$$

Integration by parts, using $\phi(a) = 0$, shows that the last term in Eq. (B13) vanishes. An evaluation of the first term, using Eq. (6.2), yields

$$K^{\psi}_{n1} = -\frac{a^2 q_n\sqrt{2\pi}}{bJ_1(q_n)\sqrt{q_n^2-1}}\frac{j_1(y_n)}{y_n} \quad \text{(TE)}, \tag{B14}$$

with $y_n = q_n a/b$. The matrix element M^{ψ}_{11} in Eq. (B7) can now be written as

$$\begin{aligned} M^{\psi}_{11} = &-\frac{2\pi a^3}{b^2 k}\sum_{n\neq N}^{\infty}{}' \tau_n a\coth\tau_n L\frac{q_n^2}{J_1^2(q_n)(q_n^2-1)}\frac{j_1^2(y_n)}{y_n^2} \\ &+\frac{2\pi k a^5}{b^2}\sum_{n\neq N}^{\infty}{}'\frac{\coth\sigma_n L}{\sigma_n a}\frac{1}{J_0^2(p_n)} \\ &\times\left[\frac{j_1(x_n)}{x_n} - \alpha j_2(x_n)\right]^2, \end{aligned} \tag{B15}$$

where

$$\sigma_n a \equiv \sqrt{x_n^2 - k^2a^2}\ , \quad \tau_n a \equiv \sqrt{y_n^2 - k^2a^2}. \tag{B16}$$

As was the case in the calculation of the polarizability, proceeding to the $a \to 0$ limit makes the sums in Eq. (B15) diverge. For small a/b, the essential contributions to the sums come from large n and we may convert the sums to integrals, with the following limiting forms constructed so as to retain the lowest two powers of k^2a^2 in M_{11}:

$$\begin{aligned} &\coth\sigma_n L \to 1\ , \quad \coth\tau_n L \to 1, \\ &J_0^2(p_n) \to \frac{2}{\pi p_n} = \frac{2a}{\pi b x_n}\ , \quad \sigma_n a \to x_n, \\ &\tau_n a \to y_n - \frac{k^2a^2}{2y_n}, \quad J_1^2(q_n) \to \frac{2a}{\pi b y_n}, \\ &\sum_n^{\infty} \to \frac{b}{\pi a}\int_0^{\infty} dx \quad \text{or} \quad \frac{b}{\pi a}\int_0^{\infty} dy. \end{aligned} \tag{B17}$$

This leads to

$$\begin{aligned} M^{\psi}_{11} &= -\frac{\pi a^2}{ka}\left\{\int_0^{\infty}\frac{dx\sqrt{x^2-k^2a^2}\,j_1^2(x)}{x}\right. \\ &\quad\left. -k^2a^2\int_0^{\infty}\frac{x\,dx}{\sqrt{x^2-k^2a^2}}\left[\frac{j_1(x)}{x} - \alpha j_2(x)\right]^2\right\} \\ &\cong -\frac{\pi a^2}{ka}\left\{\int_0^{\infty} dx\, j_1^2(x) - \frac{k^2a^2}{2}\int_0^{\infty} dx\right. \\ &\quad\left.\times\left[\frac{j_1^2(x)}{x^2} + 2\left(\frac{j_1(x)}{x} - \alpha j_2(x)\right)^2\right]\right\}, \end{aligned} \tag{B18}$$

where y has been replaced by x as the dummy variable of integration.

The general form of the integrals in Eq. (B18) is given by Watson [8]. Specifically, we use

$$\begin{aligned} &\int_0^{\infty} dx\frac{j_\mu(x)j_\nu(x)}{x^\lambda} \\ &= \frac{\pi}{2^{\lambda+2}}\frac{\Gamma\left(\frac{\mu+\nu-\lambda+1}{2}\right)}{\Gamma\left(\frac{\lambda+\mu+\nu+3}{2}\right)} \\ &\times\frac{\Gamma(\lambda+1)}{\Gamma\left(\frac{\lambda+\mu-\nu+2}{2}\right)\Gamma\left(\frac{\lambda-\mu+\nu+2}{2}\right)} \end{aligned} \tag{B19}$$

to obtain

$$\int_0^{\infty} dx j_1^2(x) = \frac{\pi}{6}, \quad \int_0^{\infty} dx\frac{j_1^2(x)}{x^2} = \frac{\pi}{15}, \tag{B20}$$

$$\int_0^{\infty} dx j_2^2(x) = \frac{\pi}{10}, \quad \int_0^{\infty} dx\frac{j_1(x)j_2(x)}{x} = \frac{\pi}{30}. \tag{B21}$$

[In fact Eq. (B20) has already been used in deriving Eq. (A19).] We then find

$$M^{\psi}_{11} = -\frac{\pi^2a^2}{6ka}\left[1 - \frac{k^2a^2}{5}(3-2\alpha+3\alpha^2)\right]. \tag{B22}$$

In order to obtain the susceptibility, we must also expand $(K^{\psi}_{N1})^2$ for small a. From Eqs. (B12) and (B14) we find

$$(K^{\psi}_{N1})^2 \cong \frac{2\pi a^4}{9b^2J_0^2(p_N)}\left[1 - \frac{p_N^2a^2}{5b^2}(1+2\alpha)\right] \quad \text{(TM)} \tag{B23}$$

and

$$(K^{\psi}_{N1})^2 \cong \frac{2\pi a^4 q_N^2}{9b^2(q_N^2-1)J_1^2(q_N)}\left[1 - \frac{q_N^2a^2}{5b^2}\right] \quad \text{(TE)}. \tag{B24}$$

To complete the calculation of $\psi_{N\ell}$, we also need $H_M^2(0)$ in Eq. (4.15) for both the $\text{TM}_{1N\ell}$ and $\text{TE}_{1N\ell}$ modes. These are found to be

$$H_M^2(0) = \frac{1}{\pi L b^2 J_0^2(p_N)} \quad \text{(TM)}, \tag{B25}$$

$$H_M^2(0) = \frac{(\ell\pi/L)^2}{\pi L b^2 k_M^2}\frac{q_N^2}{q_N^2-1}\frac{1}{J_1^2(q_N)} \quad \text{(TE)}, \tag{B26}$$

where

$$k_M^2 = k_{N\ell}^2 = p_N^2/b^2 + \ell^2\pi^2/L^2 \quad \text{(TM)}$$

or

$$q_N^2/b^2 + \ell^2\pi^2/L^2 \quad \text{(TE)}. \tag{B27}$$

Finally, we write

$$\beta_N \tan\beta_N L \cong \beta_N(\beta_N L - \ell\pi) \cong \frac{L}{2}(k^2 - k_M^2) \quad \text{(TM)}, \tag{B28}$$

$$\frac{\tan\beta_N L}{\beta_N} \cong \frac{\beta_N L - \ell\pi}{\beta_N} \cong \frac{L}{2}\left(\frac{L}{\pi\ell}\right)^2 (k^2 - k_M^2) \quad \text{(TE)}. \tag{B29}$$

In this way, Eqs. (B5) and (B6) lead to

$$\psi_{\rm TM} \cong \frac{8a^3}{3}\left[1 - \frac{p_N^2 a^2}{5b^2}(1+2\alpha) + \frac{k^2a^2}{5}(3 - 2\alpha + 3\alpha^2)\right], \tag{B30}$$

$$\psi_{\rm TE} \cong \frac{8a^3}{3}\left[1 - \frac{q_N^2 a^2}{5b^2} + \frac{k^2a^2}{5}(3 - 2\alpha + 3\alpha^2)\right]. \tag{B31}$$

The final step uses the fact that Eqs. (B30) and (B31) are variational forms with respect to the parameter α. The minimum values of $\psi_{N\ell}$ occur when

$$\alpha_{\rm TM} = \frac{1}{3} + \frac{p_N^2 a^2}{3b^2}, \quad \alpha_{\rm TE} = \frac{1}{3}, \tag{B32}$$

leading finally to

$$\psi_{\rm TM} \cong \frac{8a^2}{3}\left[1 + k^2a^2\left(\frac{8}{15} - \frac{p^2}{3k^2a^2} - \frac{p^4}{15k^4a^4}\right)\right], \tag{B33}$$

$$\psi_{\rm TE} \cong \frac{8a^2}{3}\left[1 + k^2a^2\left(\frac{8}{15} - \frac{q^2}{5k^2a^2}\right)\right], \tag{B34}$$

where

$$p \equiv p_N a/b, \quad q = q_N a/b. \tag{B35}$$

It is at first surprising that the results for a $\text{TM}_{1N\ell}$ mode and a $\text{TE}_{1N\ell}$ mode differ from each other, particularly because one would not expect the fields at the hole to be influenced by the distant cavity boundaries. But the TM and TE modes *are* different near the hole. Specifically, the primary magnetic field at the wall as described in both Eqs. (6.1) and (6.2) is in the y direction. But $\partial^2 H_y/\partial x^2$ and $\partial^2 H_y/\partial y^2$ at the wall differ for the TM and TE cavity modes. Specifically,

$$h_y^x \equiv \left.\frac{\partial^2 H_y}{\partial x^2}\right|_{\substack{x=0\\y=0}} \Big/ H_y(0) = -\frac{3p_N^2}{4b^2},$$

$$h_y^y \equiv \left.\frac{\partial^2 H_y}{\partial y^2}\right|_{\substack{x=0\\y=0}} \Big/ H_y(0) = -\frac{p_N^2}{4b^2} \quad \text{(TM)}, \tag{B36}$$

$$h_y^x = -\frac{q_N^2}{4b^2}, \; h_y^y = -\frac{3q_N^2}{4b^2} \quad \text{(TE)}, \tag{B37}$$

where $H_y(0)$ is the value of H_y that would exist at the center of the hole in the absence of a hole. Since

$$h_y^x + h_y^y = \begin{cases} -p_N^2/b^2 & \text{(TM)} \\ -q_N^2/b^2 & \text{(TE)} \end{cases} \tag{B38}$$

and

$$3h_y^x - h_y^y = \begin{cases} -2p_N^2/b^2 & \text{(TM)} \\ 0 & \text{(TE)}, \end{cases} \tag{B39}$$

we can rewrite Eq. (B30) and (B31) as

$$\psi \cong \frac{8a^3}{3}\left[1 + \frac{a^2}{5}(h_y^x + h_y^y) + \frac{k^2a^2}{5}(3 - 2\alpha + 3\alpha^2) + \frac{\alpha a^2}{5}(3h_y^x - h_y^y)\right], \tag{B40}$$

valid for either a TM or TE mode. The minimum value of ψ occurs when $6\alpha = 2 - 3h_y^x/k^2 + h_y^y/k^2$ and is

$$\psi = \frac{8a^3}{3}\left[1 + \frac{8}{15}k^2a^2 + \frac{2}{5}h_y^x a^2 + \frac{2}{15}h_y^y a^2 - \frac{(3h_y^x a^2 - h_y^y a^2)^2}{60k^2a^2}\right]. \tag{B41}$$

When we perform the complete numerical calculation of the susceptibility, as outlined in Sec. VI, we find for zero thickness that the coefficients of the lowest powers of k^2a^2 and p^2/k^2a^2,q^2/k^2a^2 agree exactly (to three significant figures) with the predicitions in Eqs. (B33) and (B34). We therefore believe that the form of ϕ in Eq. (B11) is correct. In fact, we also tried

$$\phi = \alpha x\left(1 - \frac{r^2}{a^2}\right)^{1/2} + \beta x\left(1 - \frac{r^2}{a^2}\right)^{3/2} \tag{B42}$$

and found that the minimization process led to $\beta = 0$ and α the same as in Eq. (B32).

[1] H.A. Bethe, Phys. Rev. **66**, 163 (1944).
[2] R.L. Gluckstern and F. Neri, IEEE Trans. Nucl. Sci. **NS-32**, 2403 (1985); R. L. Gluckstern, J.B.J. van Zeijts, and B. Zotter, Phys. Rev. E **47**, 656 (1993).
[3] R.E. Collin, *Field Theory of Guided Waves* (McGraw-Hill, New York, 1960).
[4] R.M. Bevensee, *Electromagnetic Slow Wave Systems* (Wiley, New York, 1964), Chap. III.

[5] C.M. Butler, Y. Rahmat-Samii, and R. Mittra, IEEE Trans. Antennas Propag. **AP-26**, 82 (1978).

[6] The analysis for a circular hole in a thick wall follows that for $k = 0$ by R.L. Gluckstern and J.A. Diamond, IEEE Trans. Microwave Theory Tech. **39**, 274 (1991), which contains references to earlier work.

[7] For $\ell = 0$, the right-hand side of both Eqs. (A21) and (A23) must be multiplied by 2, and the result in Eq. (A24) is still correct.

[8] G.N. Watson, *A Treatise on the Theory of Bessel Function*, 2nd ed. (Cambridge University Press, Cambridge, England, 1945), Sec. 13.41.

[9] W.H. Eggimann, IRE Trans. Microwave Theory Tech. **MMT-9**, 408 (1961).

[10] F. Sporleder and H.G. Unger, in *Waveguide Tapers, Transitions and Couplers*, edited by P. Peregrinus (Institute of Electrical Engineers, London, 1979).